

# CubeSense: Wireless, Battery-Free Interactivity through Low-Cost Corner Reflector Mechanisms

Xiaoying Yang  
Tongji University  
Shanghai, China  
xiaoying.yang@hotmail.com

Yang Zhang  
Carnegie Mellon University  
Pittsburgh, PA, USA  
yang.zhang@cs.cmu.edu

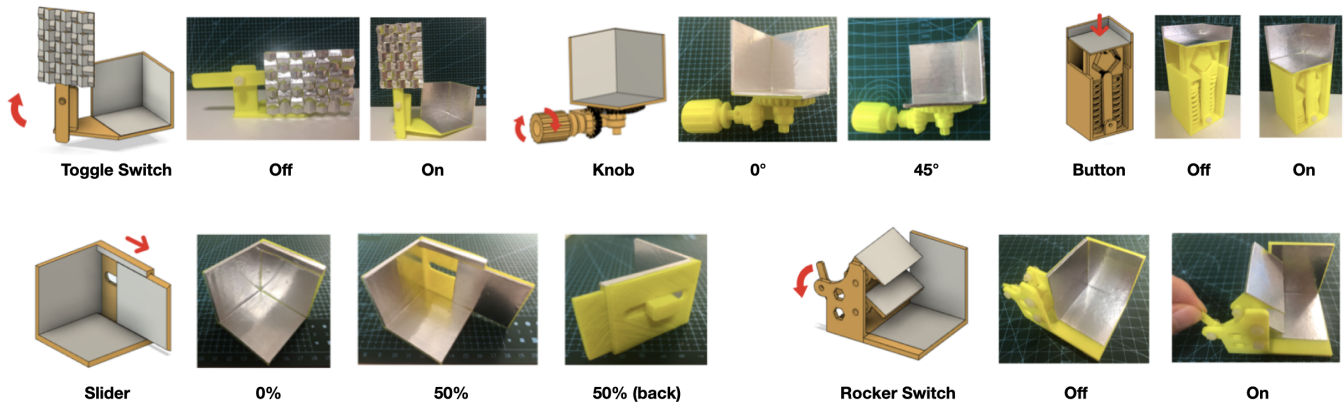


Figure 1: 3D models and close-up photos of our controllers at different states.

## ABSTRACT

Ubiquitous computing systems rely on ubiquitous methods to sense user interactions, which have manifested in our daily environments as physical buttons, switches, sliders, and beyond. These conventional controllers are either wired, which eliminates flexible deployments, or powered by batteries that require user maintenance. Additionally, built-in wireless communications such as Wi-Fi, Bluetooth, and RFID add up to the total cost. All aforementioned constraints prevent truly ubiquitous interactions from intelligent environments such as smart homes, industry 4.0, precision farming, and a wider range of Internet-of-Things (IoT) applications. We present CubeSense, a wireless and battery-free interactive sensing system which encodes user interactions into radar cross section (RCS) of corner reflectors. Through careful designs of corner reflector mechanisms, CubeSense achieves robust accuracies with controllers made of ultra-low-cost plastics and metal films, resulting in a total cost of around only 20 cents per unit.

## CCS CONCEPTS

• **Human-centered computing** → **Ubiquitous and mobile computing**; **Interaction devices**.

Permission to make digital or hard copies of all or part of this work for personal or classroom use is granted without fee provided that copies are not made or distributed for profit or commercial advantage and that copies bear this notice and the full citation on the first page. Copyrights for components of this work owned by others than ACM must be honored. Abstracting with credit is permitted. To copy otherwise, or republish, to post on servers or to redistribute to lists, requires prior specific permission and/or a fee. Request permissions from [permissions@acm.org](mailto:permissions@acm.org).

*CHI '21 Extended Abstracts, May 8–13, 2021, Yokohama, Japan*

© 2021 Association for Computing Machinery.

ACM ISBN 978-1-4503-8095-9/21/05...\$15.00

<https://doi.org/10.1145/3411763.3451599>

## KEYWORDS

Ubiquitous Computing, Internet-of-Things, Smart Environment, Millimeter Wave, Battery-free, Wireless Sensing, Fabrication

## ACM Reference Format:

Xiaoying Yang and Yang Zhang. 2021. CubeSense: Wireless, Battery-Free Interactivity through Low-Cost Corner Reflector Mechanisms. In *CHI Conference on Human Factors in Computing Systems Extended Abstracts (CHI '21 Extended Abstracts)*, May 8–13, 2021, Yokohama, Japan. ACM, New York, NY, USA, 6 pages. <https://doi.org/10.1145/3411763.3451599>

## 1 INTRODUCTION

Ubiquitous computing relies on ubiquitous interactivity through which users can easily provide input to computing resources. From remotes and controllers, to digital devices such as smart thermometers and doorbells, conventional controls have widely existed and have provided users swift and tangible controls in their environments. To power these conventional controllers, wires and batteries have been the most straightforward approach, and yet wire connection means inflexible installation, while batteries demand user effort for maintenance. Additionally, wireless communications of these controllers powered by digital transceivers such as Wi-Fi or Bluetooth contribute to the cost. All the above constraints add up to the deployment and maintenance cost of these controllers, making it challenging for truly ubiquitous deployments at scale.

In response, researchers have been exploring alternatives to build ubiquitous controllers with little effort to deploy and maintain. Prior work has investigated harnessing power from user interaction [8, 33], and environment [29, 40]. It is also possible to leverage reflector mechanisms to encode information in wireless signals,

which has been demonstrated by backscatter systems with RF waves [10, 25] and light [35].

In this work, we propose a new sensing technique based on RF reflection with corner reflector based mechanisms. We designed a variety of controllers based on these mechanisms, which encode user interactivity (e.g., button press, switch toggle, slider position, knob rotation) into RCS, in a battery-free and component-free manner. These controllers can be sensed remotely, and cost only a few cents per unit. More importantly, they do not require users to exchange batteries and demand little effort to maintain.

To achieve this, we first ran a series of simulations to verify a set of sensing principles. We then designed several controller mechanisms based on these principles, and used a 24GHz Frequency-Modulated Continuous Wave (FMCW) radar to measure their RCS in our proof-of-concept system. We conducted a preliminary study, which shows promises with an average accuracy of 91.8% for discrete controllers (i.e., buttons and switches), and 73.3% for continuous controllers (i.e., sliders and knobs). Finally, we conclude this work with discussions around example applications, limitations, and future work.

## 2 RELATED WORK

CubeSense mainly intersects with two groups of prior work: 1) sensing approaches that enable interactivity at a room-scale, and 2) interactive sensing with RF reflection.

### 2.1 Room-Scale Interactivity

Allowing users to control computing resources within their environments in a ubiquitous manner has long been sought after. There have been smart home products that allow users to install wireless battery-powered sensors for interactions with much deployment flexibility (e.g., TI SensorTag [5] and Notion [3]). Recent success in open-source hardware (e.g., Arduino) has facilitated hobbyists and makers to create custom remote controls for smart home applications. In the research domain, people leveraged mobile devices like smartphones and smartwatches for room-scale interactivity [24, 32, 37]. More relevant to our approach are previous systems that feature deployed sensors, such as cameras [19, 34], UWB transceivers [20], RFID [15, 25, 27], capacitive sensors [41, 42], and acoustic sensors [13, 14].

### 2.2 Interactive Sensing with RF Reflection

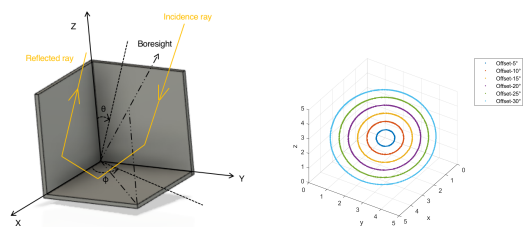
Closer to CubeSense on the technical front, are previous systems that sense radio frequency reflection for interactivity. RF sensing provides a practical path to wide-area interactive sensing with its commonly compact form factor and non-invasive sensing modality. Prior work has leveraged RF reflection off of human bodies to detect postures [6], identities [16], and even emotions [43]. It is also possible to use RF reflectors to enhance sensing performance (i.e., range, resolution, modality, and beyond). For example, Project Soli [28] first demonstrated practical applications of RF based microgesture detection. Yeo et al. [36, 38, 39] leveraged millimeter wave radars to identify tokens for tangible interactions, and objects for a wide range of context-aware applications. MechanoBeat [30] transforms mechanical energy from object uses into unique oscillations of RF reflectors for activity recognition. LiveTag [10] uses chipless Wi-Fi

tags to detect user touch. Finally, Iyer et al. [17] use Wi-Fi backscatters to create a wealth of wireless sensors such as buttons, sliders, knobs, and many more.

## 3 SENSING PRINCIPLE

Radio frequency (RF) waves reflect like other electromagnetic waves (e.g., light) when they encounter changes of mediums. In theory, the larger the conductivity difference between transmission mediums, the better their boundary reflects, which is why conductive surfaces (e.g., metal sheets) are optimum RF reflective surfaces among common everyday materials such as plastic, wood, drywall, and human body. When formed into special geometries, conductive materials can even reflect incoming RF waves back to their sources. This retro-reflectivity is important for many RF sensing applications such as communication [12], localization [18], and calibration [7]. These special geometries often consist of two or three mutually perpendicular plates (i.e., corners) which a range of incidence waves hit in sequence, and exit in a reverse direction, resulting in strong RF reflections [1, 9]. Figure 2(a) illustrates this phenomenon.

Radar Cross Section (RCS) is a measure of echo ability of targets in radar systems [22]. Interestingly, the magnitude of RCS is not only related to the physical area of corner reflectors. Within three surfaces of corner reflectors, only a specific region, called effective aperture area works for three reflections. The amount of reflected RF energy, or RCS is proportional to the magnitude of this effective aperture area. When the trihedral corner reflector is illuminated by the radar at the boresight (i.e. the symmetry axis), it often has the largest effective aperture area and therefore yields peak RCS. We recommend prior work [9, 11, 21, 23, 26] for more details. In short, the RCS of a corner reflector is a function of its material, geometry, and orientation (both azimuth  $\phi$  and elevation  $\theta$ ). Additionally, occlusions between a radar and a corner reflector could result in changes on the RCS measurements.



(a) Square trihedral corner reflector (b) Sample points around the boresight

**Figure 2: (a) With a square trihedral corner reflector, incident RF rays are reflected three times and returned back to the source.  $\phi$  and  $\theta$  are azimuth and elevation angle respectively. Boresight is aligned with the symmetry axis of the reflector. (b) Each circle comprises points that, with the origin, form vectors that share a same offset angle to the boresight. We averaged measurements across each circle for each offset angle in the simulation section.**

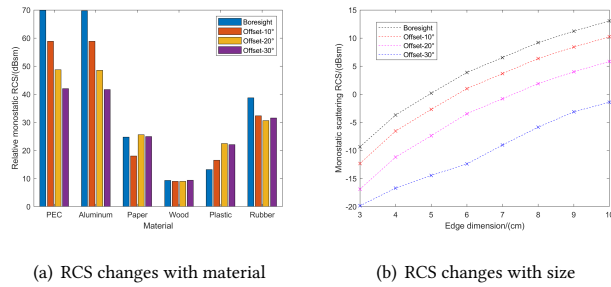


Figure 3: Mono-static RCS of a simulated square trihedral corner reflector across (a) material and (b) size.

In this work, we leverage these factors to encode user interaction with the magnitude of RCS. In fact, small changes in any of the factors around optimum conditions will result in significant changes in RCS. For example, rotating a corner reflector with its boresight pointing to a radar by a 10° elevation angle would result in a 50% reduction on RCS. Specifically, CubeSense encodes user interactions with four factors which include material, size, incidence angle, and occlusion.

To verify our sensing principle, we ran a series of simulations with CST studio [2]. Specifically, we simulated a corner reflector made of 5cm perfect-electric-conductor (PEC) squares and plotted its reflectance to excitement plane waves (24GHz). In these simulations, we varied the aforementioned factors of the corner reflector with a range of parameters, and kept track of the resulted mono-static RCS. Next, we describe the simulation setup and results in detail.

**Material** We investigated six materials with a 1mm thickness: PEC, aluminum, paper, wood, plastic, and rubber. We conducted a measurement same as the ones in the previous two investigations. Figure 3(a) shows the RCS changes, which are relative values to 70dBsm. This result confirms that metal materials have much higher RCS than non-metal materials with an average RCS improvement of 33.7dBsm.

**Size** The physical size of the corner reflector is determined by the sizes of its three surfaces. To simulate size changes on corner reflectors, we varied the edge dimension from 3 to 10cm with a 1cm increment). With each size, we measured the RCS at the boresight, and the 10°, 20°, 30° offset angle (Figure 2(b)). Figure 3(b) shows that larger corner reflectors always have higher RCS than smaller ones over all incidence angles.

**Incidence angle** As mentioned before, RCS of corner reflectors are highly dependent on the incidence angle of RF waves. We consider RCS changes with incidence angle around the boresight. Specifically, we measured the RCS at the boresight direction, and averaged the measured RCS of directions with a same offset angle, ranging from 5° to 30° with a 5° increment. Figure 4(a) shows the RCS variation with incidence angle. The average RCS continuously decreases with incidence angle deviating from the boresight, which results in a dynamic RCS range of around 15dBsm.

**Occlusion** Finally, to investigate RCS change with occlusion, we built a model with a flat PEC plate perpendicular to the boresight.

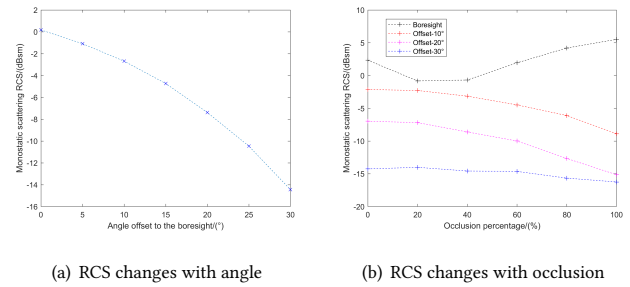


Figure 4: Mono-static RCS of a simulated square trihedral corner reflector across (a) angle and (b) occlusion.

We varied the open area to the incident RF rays by translating the PEC plate and measured the RCS with the same set of incidence angles as ones in the size investigation. The results can be seen in Figure 4(b). We found that the RCS decreases with the occlusion at all incidence angles except the boresight. This result suggests the use of RF scattering geometries or absorbing materials to attenuate reflection at the boresight in our system implementation.

## 4 DESIGN SPACE OF CUBESENSE

We know there are significant factors that change RCS of corner reflectors. Our next task is to design mechanisms that encode user interactions with these factors. We designed two types of controllers with discrete states (e.g., buttons and toggle switches) and continuous states (e.g., light dimmers and temperature knobs). Figure 1 shows these controllers.

There are two principles we leveraged in the design of corner reflector mechanisms. In the first principle, we treat the corner reflector as *a whole*. For example, we can occlude the corner reflector to invalidate its original geometry (i.e., toggle switch). We can also rotate the corner reflector to change the angle of incidence (i.e., knob). In our second principle, we change only *one surface* of the corner reflector through, translation (i.e., button and slider) and rotation (i.e., rocker switch). The change of one surface with regard to the other two leads to changes in the effective reflective area, which manifests as RCS changes. Based on these two principles, we designed several proof-of-concept mechanisms to encode user interactions into RCS of corner reflectors. To fabricate these controllers, we 3D printed their base structures out of PLA and stuck 0.1mm aluminum foils to inner surfaces to enhance their RF reflectance. We describe their designs in detail as follows.

**Toggle Switch** One straightforward approach to change RCS of the corner reflector as a whole is occluding it with RF scattering geometries. As an example, we made a toggle switch based on this mechanism. The two switch states are established by positioning the occlusion plate – RF waves are either scattered by the plate (low RCS) or retro-reflected by the corner reflector (high RCS).

**Knob** We made a knob leveraging the RCS change caused by the rotation of corner reflectors. Specifically, we used a pair of bevel gears to translate a knob's rotation into a corner reflector's rotation. When the incident RF waves are aligned with the boresight of the

reflector ( $\phi=45^\circ$ ,  $\theta=54.7^\circ$ ), the reflection is the strongest. As a user turns the knob, its RCS decreases as the corner reflector rotates.

**Push Button** In this example, we leveraged the translation motion of one surface on the corner reflector to make a button, which also features a latching mechanism. The effective reflective area to the radar is determined by the position of the movable surface. The RCS of this button is higher when the button is pressed down (on state), than when it is at the neutral position (off state).

**Slider** Similarly, we can leverage the translation of a corner reflector surface in other directions. In this example, we made a slider which controls the horizontal movement of a surface. When the surface slides away, RF reflective material is replaced by plastic and air, which do not reflect RF waves as much as the metallic surface. As a result, the RCS decreases as the slide distance increases.

**Rocker Switch** Finally, it is also possible to tilt a surface. We designed a louver-inspired mechanism with two tiltable plates forming up one surface of a corner reflector. As the plates tilt with the switch, the three-surface perpendicularity is invalidated, resulting in significant RCS decreases.

So far, we have demonstrated five designs to build controllers with discrete and continuous states based on factors that affect RCS of corner reflectors. Of course, there are more ways to encode user interactions with these factors beyond the designs we showed. For example, the knob can be replaced by a rack for implementing buttons. Moreover, mechanisms that change one surface of the corner reflector can be extended to more surfaces, enabling a wider range of flexible designs.

## 5 SYSTEM IMPLEMENTATION

### 5.1 Hardware

We built a proof-of-concept system around Infineon POSITION2GO FMCW radar operating at 24GHz [4]. At this frequency, the wavelength of the millimeter wave is around 1.25cm, which is capable of detecting objects with comparable sizes. Take the Infineon radar as an example, it can detect objects with  $RCS = 1m^2$  at a distance of 60cm-15m according the datasheet, and can detect even smaller objects at close range in practice. FMCW radar with higher frequencies can also be used for better sensitivity. The radar sensor features one transmitter (TX) and two receivers (RX). With a quadrature mixer and complex-baseband architecture implementation, the module streamed complex (I/Q) data samples output over the USB serial to a laptop for further processing.

### 5.2 Signal Processing

We built a signal processing pipeline to estimate the RCS of corner reflector controllers by monitoring the magnitude of RF reflection. According to electromagnetic field theory, RCS is proportional to received power assuming a constant distance and antenna gain [31]. In the radar system, the received spectral power can be inferred by the magnitude of beat signals. Therefore, we first apply FFT on the beat signal to obtain the range spectrum. To locate the controllers, we search peaks within a region of interest (ROI), which is acquired through user calibration. Finally, we calculate mean FFT magnitude as the indicator of RCS for further computation.

To detect discrete states of controllers (i.e., button, switch), we first record the RCS of these controllers at all states during the

calibration process, and set thresholds with mean values between states. For continuous controllers (i.e., slider, knob), we train a polynomial regression model to map RCS to a continuous output (i.e., percentage) after a similar calibration process. Our current system relies on user calibration when the controllers are first set up. However, we expect an automated process which eliminates calibration in future work.

We found that user movements can interfere with our sensing. To mitigate this interference, we compute 2D-FFT to generate a range-doppler map, with which we threshold the mean velocity. Since user movements yield high velocity as opposed to the nearly static state changes of controllers, we suspend our detection pipeline once the velocity value is higher than the threshold to avoid false positives.

### 5.3 Preliminary Evaluation

To investigate the performance of CubeSense, we ran a preliminary evaluation in an indoor environment simulating a living room setting. Particularly, we focused on three factors: distance, azimuth angle and occlusion. For each factor, we first calibrated our system, and then collected multiple rounds of detection results. Detailed procedures and results are shown as follows (Figure 5).

**Distance** We tested distances of 1m, 2m, and 3m between the controller and the radar sensor. The incident RF rays have  $0^\circ$  angle of incidence to the controller. For controllers that can be configured continuously, we defined five states (i.e., 0% to 100% with a 25% interval). On average, we achieved an accuracy of 82.2% across all distances and all types of controllers. The accuracy decreases with distance (i.e., 88.3% at 1m, 81.7% at 2m, and 76.7% at 3m), due to the path loss of the received power.

**Azimuth angle** We placed the controller in a range of horizontal azimuth angles ( $-30^\circ$ ,  $-15^\circ$ ,  $0^\circ$ ,  $15^\circ$ ,  $30^\circ$ ) at a fixed 2.5m distance to the radar sensor. The rest of the procedure was the same as the one in the distance evaluation. The average detection accuracy across all azimuth angles is 82%. We see little variance on accuracy across azimuth angles (i.e., 2% at  $0^\circ$ , 4.7% at  $\pm 15^\circ$ , and 0.3% at  $\pm 30^\circ$ ).

**Occlusion** Finally, we tested the performance of our system in non-line-of-sight (NLOS) scenarios. The radar and the controller were placed 1.5 meters apart, separated by a set of common everyday materials sequentially. These common materials included cotton fabric, plastic foam, and rubber which measured 5, 10, and 15mm thicknesses. The result indicates an average accuracy of 86.7%, 83.3%, and 81.6% across all controllers, which demonstrated a certain level of NLOS sensing capability of CubeSense.

## 6 EXAMPLE APPLICATIONS

CubeSense stands out among conventional interactive controllers for its flexible deployment, negligible maintenance, and low cost. Here we propose several examples applications that highlight these advantages of CubeSense. First, controls in physical environments such as light switches are generally fixed to a certain height on walls, which brings difficulty to children, seniors, and people with motor impairments. In response, building managers or facility owners can leverage CubeSense, to provide accessible controls. It is also possible to use CubeSense to interact with RF-enabled IoT appliances such as smart thermometers, speakers, and TV. Finally, CubeSense may

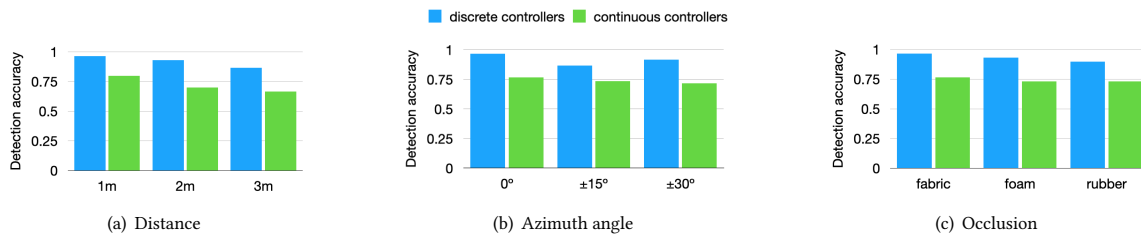


Figure 5: Detection accuracies across three factors.

be used in a wider range of controls at public places such as pull cords on buses, caregiver pager, restaurant table call systems, and beyond.

## 7 LIMITATION AND FUTURE WORK

First, CubeSense requires user calibration by manually defining ROI and adjusting the threshold to determine controller states. If controllers are moved or if the environment configuration is changed, users will have to recalibrate the system. We plan to eliminate this labor by improving our sensing approach with higher spatial resolutions and a dynamic thresholding to automatically locate controllers in environments and recognize their states.

Another limitation is around the line-of-sight detection. Although our evaluation results demonstrate preliminary sensing capabilities under occlusions, CubeSense cannot sense through thick conductive materials such as walls mostly because of our high operation frequency (i.e., 24GHz). To address this limitation in the future, we plan to leverage radar sensing with multiple frequencies.

Finally, it is possible to miniaturize our controllers with better fabrications that yield smoother surfaces and by leveraging multiple materials including ones that absorb RF waves. In addition, future work will aim for better human-machine ergonomics with mechanical designs tailored to real-world applications.

## 8 CONCLUSION

We present CubeSense, a low-cost, wireless, and battery-free sensing system that enables ubiquitous interactivity in a tangible manner. By leveraging the retro-reflectivity of corner reflectors, we create several proof-of-concept controllers which encode user interactions into their RCS for remote detection by radars. These controllers are made of only plastics and metal films which can be extremely low-cost. The battery-free and component-free nature of these controllers significantly lowers the need for user maintenance. We conducted a series of simulations and preliminary evaluations to demonstrate the feasibility of our approach. Overall, CubeSense introduces a promising direction for future IoT, smart environments, and ubiquitous computing applications.

## REFERENCES

- [1] 1980. IEEE Standard Dictionary of Electrical and Electronics Terms. *IEEE Transactions on Power Apparatus and Systems* PAS-99, 6 (1980), 37a–37a.
- [2] CST n.d. *CST STUDIO SUITE, Software Information*. CST. <https://www.3ds.com/products-services/simulia/products/cst-studio-suite> Accessed Oct. 8, 2020.
- [3] Notion n.d. *Notion, Product Information*. Notion. <https://getnotion.com> Accessed Oct. 8, 2020.
- [4] Infineon n.d. *POSITION2GO*. Infineon. <https://www.infineon.com/cms/en/product/evaluation-boards/demo-position2go/> Accessed Oct. 8, 2020.
- [5] Texas Instruments n.d. *Texas Instruments, Product Information*. Texas Instruments. <https://www.ti.com/tool/TIDC-CC2650STK-SENSORIAG> Accessed Oct. 8, 2020.
- [6] Fadel Adib and Dina Katabi. 2013. See through walls with WiFi!. In *ACM SIGCOMM 2013 Conference, SIGCOMM'13, Hong Kong, China, August 12–16, 2013*, Dah Ming Chiu, Jia Wang, Paul Barford, and Srinivasan Seshan (Eds.). ACM, 75–86. <https://doi.org/10.1145/2486001.2486039>
- [7] D. J. Crisp. 2018. Robust Absolute Calibration for SAR. In *2018 International Conference on Radar (RADAR)*. 1–6. <https://doi.org/10.1109/RADAR.2018.8557317>
- [8] Jasper de Winkel, Vito Kortbeek, Josiah D. Hester, and Przemyslaw Pawelczak. 2020. Battery-Free Game Boy. *Proc. ACM Interact. Mob. Wearable Ubiquitous Technol.* 4, 3 (2020), 111:1–111:34. <https://doi.org/10.1145/3411839>
- [9] HD Eckhardt. 1971. Simple model of corner reflector phenomena. *Applied Optics* 10, 7 (1971), 1559–1566. <https://doi.org/10.1364/AO.10.001559>
- [10] Chuhan Gao, Yilong Li, and Xinyu Zhang. 2018. LiveTag: Sensing Human-Object Interaction through Passive Chipless WiFi Tags. In *15th USENIX Symposium on Networked Systems Design and Implementation, NSDI 2018, Renton, WA, USA, April 9–11, 2018*, Sujata Banerjee and Srinivasan Seshan (Eds.). USENIX Association, 533–546. <https://www.usenix.org/conference/nsdi18/presentation/gao>
- [11] Jos Groot. 1992. Letter: Cross Section Computation of Trihedral Corner Reflectors with the Geometrical Optics Approximation. *Eur. Trans. Telecommun.* 3, 6 (1992), 637–642. <https://doi.org/10.1002/ett.4460030618>
- [12] Devi S. Gunawan, Lih-Yuan Lin, and Kristofer S.J. Pister. 1995. Micromachined corner cube reflectors as a communication link. *Sensors and Actuators A: Physical* 47, 1 (1995), 580 – 583. [https://doi.org/10.1016/0924-4247\(94\)00966-L](https://doi.org/10.1016/0924-4247(94)00966-L)
- [13] Chris Harrison and Scott E. Hudson. 2008. Scratch input: creating large, inexpensive, unpowered and mobile finger input surfaces. In *Proceedings of the 21st Annual ACM Symposium on User Interface Software and Technology, Monterey, CA, USA, October 19–22, 2008*, Steve B. Cousins and Michel Beaudouin-Lafon (Eds.). ACM, 205–208. <https://doi.org/10.1145/1449715.1449747>
- [14] Chris Harrison, Robert Xiao, and Scott E. Hudson. 2012. Acoustic barcodes: passive, durable and inexpensive notched identification tags. In *The 25th Annual ACM Symposium on User Interface Software and Technology, UIST '12, Cambridge, MA, USA, October 7–10, 2012*, Rob Miller, Hrvoje Benko, and Celine Latulipe (Eds.). ACM, 563–568. <https://doi.org/10.1145/2380116.2380187>
- [15] Meng-Ju Hsieh, Jr-Ling Guo, Chin-Yuan Lu, Han-Wei Hsieh, Rong-Hao Liang, and Bing-Yu Chen. 2019. RFTouchPads: Batteryless and Wireless Modular Touch Sensor Pads Based on RFID. In *Proceedings of the 32nd Annual ACM Symposium on User Interface Software and Technology, UIST 2019, New Orleans, LA, USA, October 20–23, 2019*, François Guimbretière, Michael Bernstein, and Katharina Reinecke (Eds.). ACM, 999–1011. <https://doi.org/10.1145/3332165.3347910>
- [16] Chen-Yu Hsu, Rumen Hristov, Guang-He Lee, Mingmin Zhao, and Dina Katabi. 2019. Enabling Identification and Behavioral Sensing in Homes using Radio Reflections. In *Proceedings of the 2019 CHI Conference on Human Factors in Computing Systems, CHI 2019, Glasgow, Scotland, UK, May 04–09, 2019*, Stephen A. Brewster, Geraldine Fitzpatrick, Anna L. Cox, and Vassilis Kostakos (Eds.). ACM, 548. <https://doi.org/10.1145/3290605.3300778>
- [17] Vikram Iyer, Justin Chan, and Shyamnath Gollakota. 2017. 3D printing wireless connected objects. *ACM Trans. Graph.* 36, 6 (2017), 242:1–242:13. <https://doi.org/10.1145/3130800.3130822>
- [18] A. Jiménez-Sáez, M. Schüßler, M. El-Absi, A. A. Abbas, K. Solbach, T. Kaiser, and R. Jakoby. 2020. Frequency Selective Surface Coded Retroreflectors for Chipless Indoor Localization Tag Landmarks. *IEEE Antennas and Wireless Propagation Letters* 19, 5 (2020), 726–730. <https://doi.org/10.1109/LAWP.2020.2975143>
- [19] Brett R. Jones, Rajinder Sodhi, Michael Murdock, Ravish Mehra, Hrvoje Benko, Andrew Wilson, Eyal Ofek, Blair MacIntyre, Nikunj Raghuvanshi, and Lior Shapira. 2014. RoomAlive: magical experiences enabled by scalable, adaptive projector-camera units. In *The 27th Annual ACM Symposium on User Interface Software and Technology, UIST '14, Honolulu, HI, USA, October 5–8, 2014*,

- Hrvoje Benko, Mira Dontcheva, and Daniel Wigdor (Eds.). ACM, 637–644. <https://doi.org/10.1145/2642918.2647383>
- [20] Runchang Kang, Anhong Guo, Gierad Laput, Yang Li, and Xiang 'Anthony' Chen. 2019. Minuet: Multimodal Interaction with an Internet of Things. In *Symposium on Spatial User Interaction (SUI '19)*. ACM, New York, NY, USA, 2:1–2:10. <https://doi.org/10.1145/3357251.3357581>
- [21] KM Keen. 1983. New technique for the evaluation of the scattering cross-sections of radar corner reflectors. In *IEEE Proceedings H (Microwaves, Optics and Antennas)*, Vol. 130. IET, 322–326. <https://doi.org/10.1049/ip-h-1.1983.0054>
- [22] Eugene F Knott. 2012. *Radar cross section measurements*. Springer Science & Business Media.
- [23] Sandia National Laboratories, United States. Department of Energy. Office of Scientific, and Technical Information. 2008. *Reflectors for SAR Performance Testing*. United States. Department of Energy. <https://books.google.co.jp/books?id=uK5gAQAACAAJ>
- [24] Gierad Laput, Robert Xiao, and Chris Harrison. 2016. ViBand: High-Fidelity Bio-Acoustic Sensing Using Commodity Smartwatch Accelerometers. In *Proceedings of the 29th Annual Symposium on User Interface Software and Technology, UIST 2016, Tokyo, Japan, October 16-19, 2016*, Jun Rekimoto, Takeo Igarashi, Jacob O. Wobbrock, and Daniel Avrahami (Eds.). ACM, 321–333. <https://doi.org/10.1145/2984511.2984582>
- [25] Hanchuan Li, Eric Brockmeyer, Elizabeth J. Carter, Josh Fromm, Scott E. Hudson, Shwetak N. Patel, and Alanson P. Sample. 2016. PaperID: A Technique for Drawing Functional Battery-Free Wireless Interfaces on Paper. In *Proceedings of the 2016 CHI Conference on Human Factors in Computing Systems, San Jose, CA, USA, May 7-12, 2016*, Jofish Kaye, Allison Druin, Cliff Lampe, Dan Morris, and Juan Pablo Hourcade (Eds.). ACM, 5885–5896. <https://doi.org/10.1145/2858036.2858249>
- [26] Hsueh-Jyh Li and Yean-Woei Kiang. 2005. 10 - Radar and Inverse Scattering. In *The Electrical Engineering Handbook*, WAI-KAI CHEN (Ed.). Academic Press, Burlington, 671 – 690. <https://doi.org/10.1016/B978-012170960-0/50047-5>
- [27] Rong-Hao Liang, Meng-Ju Hsieh, Jheng-You Ke, Jr-Ling Guo, and Bing-Yu Chen. 2018. RFIMatch: Distributed Batteryless Near-Field Identification Using RFID-Tagged Magnet-Biased Reed Switches. In *The 31st Annual ACM Symposium on User Interface Software and Technology, UIST 2018, Berlin, Germany, October 14-17, 2018*, Patrick Baudisch, Albrecht Schmidt, and Andy Wilson (Eds.). ACM, 473–483. <https://doi.org/10.1145/3242587.3242620>
- [28] Jaime Lien, Nicholas Gillian, Mustafa Emre Karagozler, Patrick Amihood, Carsten Schwesig, Erik Olson, Hakim Raja, and Ivan Poupyrev. 2016. Soli: ubiquitous gesture sensing with millimeter wave radar. *ACM Trans. Graph.* 35, 4 (2016), 142:1–142:19. <https://doi.org/10.1145/2897824.2925953>
- [29] Yogesh Kumar Meena, Krishna Seunarine, Deepak Ranjan Sahoo, Simon Robinson, Jennifer Pearson, Chi Zhang, Matt Carnie, Adam Pockett, Andrew Prescott, Suzanne K. Thomas, Harrison Ka Hin Lee, and Matt Jones. 2020. PV-Tiles: Towards Closely-Coupled Photovoltaic and Digital Materials for Useful, Beautiful and Sustainable Interactive Surfaces. In *CHI '20: CHI Conference on Human Factors in Computing Systems, Honolulu, HI, USA, April 25-30, 2020*, Regina Bernhaupt, Florian 'Floyd' Mueller, David Verweij, Josh Andres, Joanna McGrenere, Andy Cockburn, Ignacio Avellino, Alix Goguey, Pernille Bjøn, Shengdong Zhao, Briane Paul Samson, and Rafal Kocielnik (Eds.). ACM, 1–12. <https://doi.org/10.1145/3313831.3376368>
- [30] Md. Farhan Tasnim Oshim, Julian Killingback, Dave Follette, Huaishu Peng, and Tauhidur Rahman. 2020. MechanoBeat: Monitoring Interactions with Everyday Objects using 3D Printed Harmonic Oscillators and Ultra-Wideband Radar. In *UIST '20: The 33rd Annual ACM Symposium on User Interface Software and Technology, Virtual Event, USA, October 20-23, 2020*, Shamsi T. Iqbal, Karon E. MacLean, Fanny Chevalier, and Stefanie Mueller (Eds.). ACM, 430–444. <https://doi.org/10.1145/3379337.3415902>
- [31] M.A. Richards. 2005. *Fundamentals Of Radar Signal Processing*. McGraw-Hill Education (India) Pvt Limited. <https://books.google.com.hk/books?id=qizdSv8MEngC>
- [32] Lei Shi, Maryam Ashoori, Yunfeng Zhang, and Shiri Azenkot. 2018. Knock knock, what's there: converting passive objects into customizable smart controllers. In *Proceedings of the 20th International Conference on Human-Computer Interaction with Mobile Devices and Services, MobileHCI 2018, Barcelona, Spain, September 03-06, 2018*, Lynne Baillie and Nuria Oliver (Eds.). ACM, 31:1–31:13. <https://doi.org/10.1145/3229434.3229453>
- [33] Nicolas Villar and Steve Hodges. 2010. The peppermill: a human-powered user interface device. In *Proceedings of the 4th International Conference on Tangible and Embedded Interaction 2010, Cambridge, MA, USA, January 24-27, 2010*, Marcelo Coelho, Jamie Zigelbaum, Hiroshi Ishii, Robert J. K. Jacob, Pattie Maes, Thomas Pederson, Orit Shaer, and Ron Wakkary (Eds.). ACM, 29–32. <https://doi.org/10.1145/1709886.1709893>
- [34] Robert Xiao, Chris Harrison, and Scott E. Hudson. 2013. WorldKit: rapid and easy creation of ad-hoc interactive applications on everyday surfaces. In *2013 ACM SIGCHI Conference on Human Factors in Computing Systems, CHI '13, Paris, France, April 27 - May 2, 2013*, Wendy E. Mackay, Stephen A. Brewster, and Susanne Bødker (Eds.). ACM, 879–888. <https://doi.org/10.1145/2470654.2466113>
- [35] Xieyang Xu, Yang Shen, Junrui Yang, Chenren Xu, Guobin Shen, Guojun Chen, and Yunzhe Ni. 2017. PassiveVLC: Enabling Practical Visible Light Backscatter Communication for Battery-free IoT Applications. In *Proceedings of the 23rd Annual International Conference on Mobile Computing and Networking, MobiCom 2017, Snowbird, UT, USA, October 16 - 20, 2017*, Kobus van der Merwe, Ben Greenstein, and Kannan Srinivasan (Eds.). ACM, 180–192. <https://doi.org/10.1145/3117811.3117843>
- [36] Hui-Shyong Yeo, Gergely Flamich, Patrick Schrempf, David Harris-Birtill, and Aaron Quigley. 2016. RadarCat: Radar Categorization for Input & Interaction. In *Proceedings of the 29th Annual Symposium on User Interface Software and Technology, UIST 2016, Tokyo, Japan, October 16-19, 2016*, Jun Rekimoto, Takeo Igarashi, Jacob O. Wobbrock, and Daniel Avrahami (Eds.). ACM, 833–841. <https://doi.org/10.1145/2984511.2984515>
- [37] Hui-Shyong Yeo, Juyoung Lee, Hyung-il Kim, Aakar Gupta, Andrea Bianchi, Daniel Vogel, Hideki Koike, Woontack Woo, and Aaron Quigley. 2019. WRIST: Watch-Ring Interaction and Sensing Technique for Wrist Gestures and Macro-Micro Pointing. In *Proceedings of the 21st International Conference on Human-Computer Interaction with Mobile Devices and Services, MobileHCI 2019, Taipei, Taiwan, October 1-4, 2019*. ACM, 19:1–19:15. <https://doi.org/10.1145/3338286.3340130>
- [38] Hui-Shyong Yeo, Ryosuke Minami, Kirill Rodriguez, George Shaker, and Aaron Quigley. 2018. Exploring Tangible Interactions with Radar Sensing. *Proc. ACM Interact. Mob. Wearable Ubiquitous Technol.* 2, 4 (2018), 200:1–200:25. <https://doi.org/10.1145/3287078>
- [39] Hui-Shyong Yeo and Aaron Quigley. 2018. Radar sensing in human-computer interaction. *Interactions* 25, 1 (2018), 70–73. <https://doi.org/10.1145/3159651>
- [40] Dingtian Zhang, Jung Wook Park, Yang Zhang, Yuhui Zhao, Yiyang Wang, Yunzhi Li, Tanvi Bhagwat, Wen-Fang Chou, Xiaojia Jia, Bernard Kippelen, Canek Fuentes-Hernandez, Thad Starner, and Gregory D. Abowd. 2020. OptoSense: Towards Ubiquitous Self-Powered Ambient Light Sensing Surfaces. *Proc. ACM Interact. Mob. Wearable Ubiquitous Technol.* 4, 3 (2020), 103:1–103:27. <https://doi.org/10.1145/3411826>
- [41] Yang Zhang, Gierad Laput, and Chris Harrison. 2017. Electrick: Low-Cost Touch Sensing Using Electric Field Tomography. In *Proceedings of the 2017 CHI Conference on Human Factors in Computing Systems, Denver, CO, USA, May 06-11, 2017*, Gloria Mark, Susan R. Fussell, Cliff Lampe, m. c. schraefel, Juan Pablo Hourcade, Caroline Appert, and Daniel Wigdor (Eds.). ACM, 1–14. <https://doi.org/10.1145/3025453.3025842>
- [42] Yang Zhang, Chouchang (Jack) Yang, Scott E. Hudson, Chris Harrison, and Alanson P. Sample. 2018. Wall++: Room-Scale Interactive and Context-Aware Sensing. In *Proceedings of the 2018 CHI Conference on Human Factors in Computing Systems, CHI 2018, Montreal, QC, Canada, April 21-26, 2018*, Regan L. Mandryk, Mark Hancock, Mark Perry, and Anna L. Cox (Eds.). ACM, 273. <https://doi.org/10.1145/3173574.3173847>
- [43] Mingmin Zhao, Fadel Adib, and Dina Katabi. 2016. Emotion recognition using wireless signals. In *Proceedings of the 22nd Annual International Conference on Mobile Computing and Networking, MobiCom 2016, New York City, NY, USA, October 3-7, 2016*, Yingying Chen, Marco Gruteser, Y. Charlie Hu, and Karthik Sundaresan (Eds.). ACM, 95–108. <https://doi.org/10.1145/2973750.2973762>